2014

Numerical Simulation Of 3D Flow In Right-Angled Confluences With Bed Elevation Discordance In The Main River

Dejana Đorđević

11th International Conference on Hydroinformatics
HIC 2014, New York City, USA

NUMERICAL SIMULATION OF 3D FLOW AT RIGHT-ANGLED CONFLUENCES WITH BED ELEVATION DISCORDANCE IN THE MAIN RIVER

DEJANA ĐORĐEVIĆ
Faculty of Civil Engineering, University of Belgrade, Bulevar kralja Aleksandra 73, 11000 Belgrade,Serbia

This paper studies flow characteristics in a right-angled confluence when the difference in bed elevations (Δz_{MR}) is created at the entrance of the upstream stretch of the main-river to the confluence. To do this a 3D finite-volume model with the k-ε turbulence model closure is used. Four values of the bed elevation discordance ratio are considered: $\Delta z_{MR}/h_d = \{0.00, 0.10, 0.25, 0.50\}$, where $\Delta z_{MR} = 0.00$ corresponds to the concordant beds' case. Numerical simulation results have shown that the presence of the bed-step lower than $0.10h_d$ hardly affects the flow pattern within the confluence. When $\Delta z_{MR} \geq 0.25h_d$ the following is observed: 1) a portion of the tributary flow is withdrawn towards the bed-step, due to a large pressure drop in front of the bed-step, 2) the difference in bed elevations creates a strong 3D flow within the confluence, 3) the w-velocity reaches the same order of magnitude as the horizontal velocity V_{xy}, 4) the strong upward motion exists along the opposite wall/bank 3−5 canal widths downstream of the confluence thus endangering its stability and 5) the shape of the recirculation zone is preserved, but the size is reduced by 20% for $\Delta z_{MR} = 0.50h_d$.

INTRODUCTION

Two major morphological phenomena in alluvial river confluences are the development of an avalanche face or faces at the entrance of one or both converging channels to the confluence, and deepening of the scour hole in the post-confluence channel (PCC). The avalanche faces are developed due to a deposition of coarser sediments that arrive from these channels and their corresponding catchments. The development of an avalanche face creates the difference in bed elevations between the incoming and outgoing channels. Laboratory experiments in movable bed models of confluences (Best [1], Mosley [11], Weerakoon et al. [14]) showed, and bathymetric surveys in field confluences (De Serres *et al*. [4], Đorđević [5], Kennedy [10]) confirmed, that avalanche faces develop in both converging channels only in alluvial river confluences with large junction angles ($\alpha \geq 45^o$).

It was shown in the author's previous works (Đorđević [6 and 7]) that the difference in bed elevations between the converging and outgoing channels is one of the major controls to the complicated, 3D flow pattern in a river confluence. However, only the effect of the bed elevation discordance between the tributary and main channels was studied. The effect of bed elevation discordance in the main river in an asymmetrical confluence has not yet been studied. This paper, thus, continues the line of the author's previous investigations by considering the effect of different extents of bed elevation discordance in the main river ($\Delta z_{MR} / h_d$) on the flow characteristics in the

confluence hydrodynamics zone (CHZ, Fig. 1b). The difference in bed elevations between stretches of the main river that extend upstream and downstream of the upstream junction corner is denoted by Δz_{MR} and the flow depth in the main river at the confluence, by h_d (Fig. 2). To facilitate a comparison with the previous studies and to follow the above mentioned findings regarding the limit junction angle, only the straight-channels' confluence with the junction angle $\alpha = 90^{o}$ is considered. The confluence layout and channels' geometries from the Shumate's physical model of a confluence [13] (Fig. 1a) are used again as the starting point for the study. This time, the upstream stretch of the main canal is successively elevated from $\Delta z_{MR} = 0$ (concordant beds' confluence – CB' confluence) to $\Delta z_{MR} = 0.5 h_d$ (discordant beds' confluence – DB's confluence, Fig. 2) to give four different confluence layouts (Table 1).

The role of bed elevation discordance in the main river is studied in the same manner as in the previous studies, i.e. by observing: 1) variations of flow angles in the flow deflection zone (Fig. 1), 2) cross-sectional distributions of the three velocity components in the confluence and the PCC, and 3) variations of the recirculation zone (RZ) size throughout the flow depth.

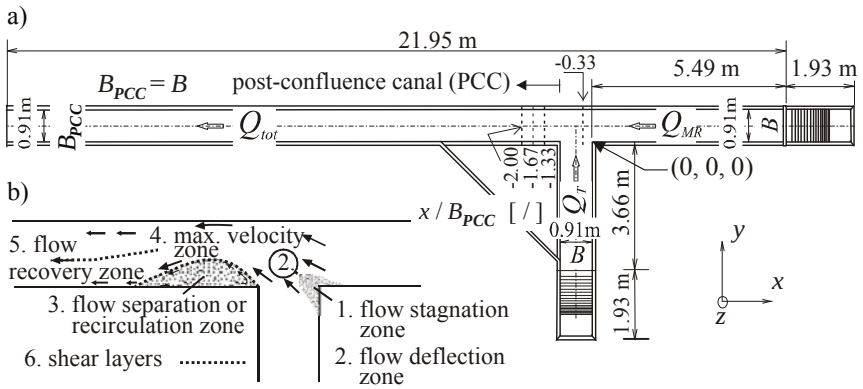

Figure 1. a) Plan-view of the Shumate's laboratory confluence (Shumate [13]), b) distribution of six subzones within the confluence hydrodynamics zone after Best [1] (from Đorđević [6])

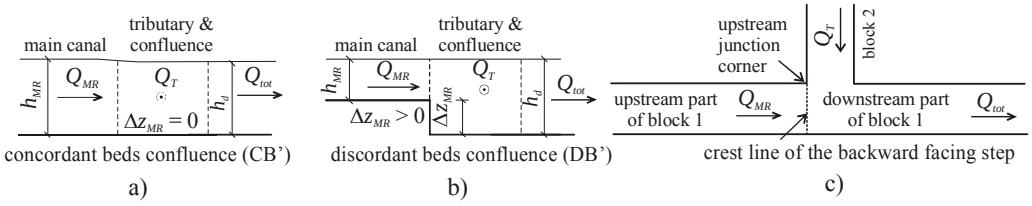

Figure 2. Definition sketches for the: a) concordant and b) discordant beds' confluence and c) division of the computational domain into blocks with the indicated position of the bed-step which divides block 1 into upstream (shallower) and downstream (deeper) parts

Table 1. Case descriptions and corresponding grid sizes of the upstream part of block 1

Case No.	$\Delta z_{MR} / h_d$ [/]	Grid size of the upstream part of block 1	Case description
1	0.00	220 × 38 ×21	concordant beds' confluence
2	0.10	220 × 38 ×19	discordant beds' confluence
3	0.25	220 × 38 ×16	
4	0.50	220 × 38 ×11	

EXPERIMENTAL SETUP

As it was already mentioned, this study rests on the geometrical and hydraulic data from the Shumate's concordant beds' confluence, whose layout is presented in Figure 1. The facility was originally used to collect data for 3D numerical model testing (Huang *et al*. [9]). These data were also used to validate 3D numerical that is applied in this study (Đorđević [5 and 6]), as they have six velocity datasets each of which contains instantaneous (u, v, w) data from 2850 measurement points. The datasets cover a range of possible hydrological scenarios in the confluence, that are defined by the discharge ratio $D_R = Q_{MR}/Q_{tot}$. The total discharge (Q_{tot}) of 0.17 m^3/s was the same in all experiments.

To keep up with the previous studies, the hydraulic data pertaining to the experiment with $D_R = 0.583$, are chosen for the present analysis. The main reason for such a choice is the fact that all six CHZ regions (Fig. 1b) are developed under this scenario.

NUMERICAL MODELLING

The numerical study of the 3D flow in the CHZ is performed using the same numerical model that was previously used to analyse the role of the difference in bed elevations between the tributary and main canals. This is the SSIIM2 model (Olsen [12]). The SSIIM2 is a 3D finite-volume based model that solves Reynolds-averaged Navier-Stokes equations using the two-equation turbulence model closure. Several versions of the k-ε-type model are available for solving RANS equations. However, comparison with the Shumate's experimental data, during the model validation procedure, has shown that the standard k-ε model has the best overall performance (Đorđević [5 and 6]). Thus, all simulations are performed using this type of the k-ε model. The coupling of the continuity and momentum equations in SSIIM2 is achieved using the SIMPLE algorithm.

The SSIIM2 model can solve governing equations on a multi-block grid. This is especially important for river confluence modelling, since the confluence plan-view is dendritic in shape. Due to large velocity and pressure gradients, which develop in the confluence, the convective terms in the momentum equations are discretised using the second-order upwind scheme.

Since the Shumate's experiments were performed under the steady and subcritical flow conditions, all numerical simulations in this paper are based on assumptions that the flow is steady and subcritical. The free-surface is treated as a rigid-lid, because the SSIIM2 has no option to use a porosity approach. However, such a treatment of the free-surface did not deteriorate the agreement between the simulation results and the measurements (Đorđević [5 and 6]).

As far as the boundary conditions are concerned, the symmetric boundary condition in the normal velocity component is used at both open boundaries – the free-surface and the outflow boundary, and the wall-law is used at the solid boundary (riverbed and banks). Constant fluxes are prescribed at inflow boundaries, and the constant depth is prescribed at the outflow boundary.

The limits of the computational domain coincide with the inflow and outflow cross-sections in the Shumate's facility (Fig. 1a). With such a positioning of the domain boundaries, it is expected that they have no influence on the flow pattern in the CHZ. The domain is covered with two orthogonal structured grids or blocks. The block 1 covers the main canal and the block 2 covers the tributary canal (Fig. 2c). The size of the block 1 differs in the concordant and discordant beds' layouts due to the presence of the backward facing step at the entrance of the upstream part of the main canal to the confluence (Fig. 2). More precisely, the size of that part of block 1, which extends downstream of the backward facing step (BS), is the same regardless the confluence layout (CB' or DB' confluence) – it has 658 × 38 × 21 cells. These digits indicate a number of cells in the downstream, lateral and vertical directions, respectively. The same holds for the size of block 2, which has 183 × 38 × 21 cells. However, that part of the block 1, which extends upstream of the back-step, changes its size as the extent of the bed elevation discordance ($\Delta z_{MR} / h_d$) increases (Table 1).

RESULTS AND DISCUSSION

The presentation and discussion of numerical simulation results starts in the flow deflection zone, where the CHZ begins (Fig. 1b). This is the area where the transfer of momentum from the tributary to the main canal takes place. Flow angles δ = arc tg (v/u) and φ = arc tg [($u^2 + v^2$)/w] in the downstream tributary cross-section indicate how the total momentum from the tributary is distributed, i.e. weather a bulk of momentum is transferred in the horizontal (δ-angle) or in the vertical direction (φ-angle). To see how the presence of the BS affects this transfer, distributions of the δ and φ angles along junction lines, that connect upstream and downstream junction corners (see definition sketch at the bottom of Figure 3) at different elevations above the tributary bed, are, therefore, examined first. Consequently, influence of Δz_{MR} on the flow characteristics in the confluence and the PCC is assessed through the analyses of cross-sectional distributions of the three velocity components within the confluence and the PCC, and variations of the RZ size throughout the flow depth.

Flow angles. Distributions of flow angles δ and φ at several non-dimensional elevations above the tributary bed are presented in Figure 3. As it was intuitively expected, the presence of the BS in the main canal ($\Delta z_{MR} \geq 0.10 h_d$) helps the tributary flow to keep its original direction ($\delta \approx \alpha$) within the narrow zone close to the upstream junction corner ($l \leq 0.10 L_{u\text{-}d}$, Fig. 3a), because its face lies in the same plane as the tributary wall. The original flow direction is kept only below the BS crest ($z < \Delta z_{MR}$). However, when the BS is higher than $0.25 h_d$, a large pressure drop develops below the step (case 4, Fig. 4). This pressure drop causes redirection of one portion of the tributary flow towards the BS (case 4, Fig. 4). Consequently, the δ-angle values in the narrow zone close to the upstream junction corner are larger than the junction angle α (Fig. 3a). The width of the zone of the redirected tributary flow reduces with the distance from the channel bed ($0.25 L_{u\text{-}d}$ at $z = 0.008 h_T$ and $0.15 L_{u\text{-}d}$ at

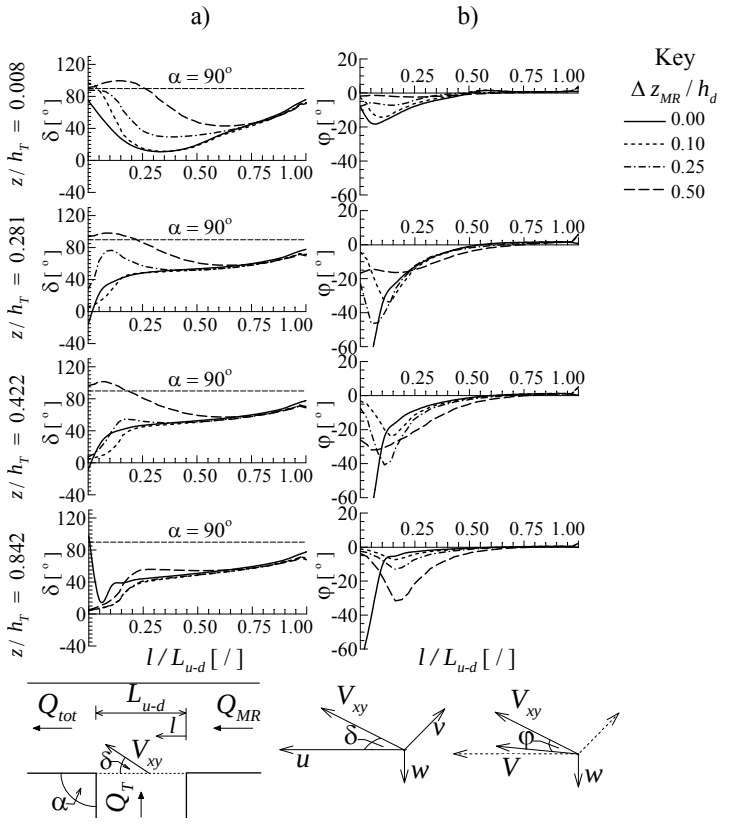

Figure 3. Variations of: a) δ and b) φ angles along junction lines at different elevations above the tributary bed

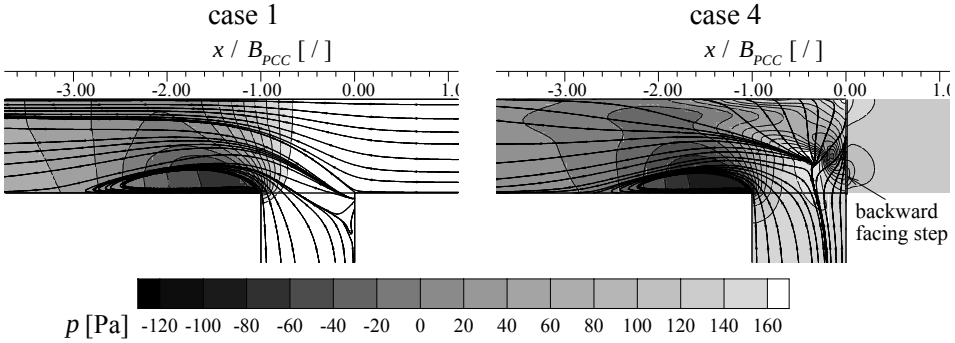

Figure 4. Effects of bed elevation discordance in the main-canal on the flow deflection on the horizontal plane and the size of RZ; streamlines near bottom (z / h = 0.008) are superimposed on pressure distributions at the bottom

$z = 0.422h_T$, Fig. 3a). This area might be understood as the zone of influence of the BS on the tributary flow. Within this area the maximum δ-angle values are attained at $0.14L_{u\text{-}d}$, near the bottom ($z = 0.008h_T$), and at $0.08L_{u\text{-}d}$, for $z > 0.50\Delta z_{MR}$. The corresponding minima are located approximately at $0.65L_{u\text{-}d}$.

Above the BS crest-level ($z > \Delta z_{MR}$) the tributary flow turns downstream under the influence of that part of the main-canal flow which is not affected by the presence of the BS, meaning that $\delta < \alpha$ throughout the junction-line, as in the CB' confluences (case 1, Fig. 4). From $z = \Delta z_{MR}$, the δ-lines gradually become monotonously rising curves with the lowest δ-angle values (2º – 3º) at the upstream junction corner, where the two flows collide.

The vertical flow deflection at the tributary entrance to the confluence is presented in Figure 3b. It is readily noticeable that the strongest vertical deflection, i.e. the strongest 3D flow is confined to the upstream half of the junction line, regardless the Δz_{MR}-value. The tributary flow is directed downwards in this part of the cross-section due to its collision with the main-canal flow (thus the negative φ-angle values). However, the presence of the BS in the main canal attenuates 3D flow near the upstream junction corner in the layers below the BS-crest ($z < \Delta z_{MR}$), because there is no direct collision between the two converging flows there. Close to the bottom (z / h = 0.008) the lowest vertical deflection of the tributary flow is recorded for $\Delta z_{MR} = 0.50$ and the highest for $\Delta z_{MR} = 0.00$. In terms of absolute values, the maximum φ-angle value for $\Delta z_{MR} = 0.50$ is approximately 10 times smaller than that from the CB' confluence. The absolute φ-angle values increase with distance from the tributary bed. The direct collision of the two flows begins at the BS-crest, where $|\varphi|_{max}$ is reached for each DB' confluence layout. The situation in the upper half of the water column (z / h = 0.824, Fig 3b) is quite the opposite to that near the bottom – the greatest vertical deflection is recorded in the confluence with the largest extent of the bed elevation discordance ($\Delta z_{MR} = 0.50h_d$). However, the absolute maximum is still smaller than that in the CB' confluence. It is also worth mentioning that the $|\varphi|_{max}$ is reached within $0.15L_{u\text{-}d}$ in the lower half of the water column. In the upper half, φ-peaks move downstream, but never further than $0.20L_{u\text{-}d}$. The φ-angle changes its sign, i.e. becomes positive, between $0.50L_{u\text{-}d}$ and $0.90L_{u\text{-}d}$, depending on the Δz_{MR}-value. However, in terms of absolute values, these positive φ-angle values are much smaller than the negative ones. This means that the tributary flow is practically two-dimensional near the downstream junction corner.

Cross-sectional velocity distributions for the three velocity components are presented in Figure 5. Those for vertical (w) and lateral (v) velocities in the confluence ($x/B_{PCC} = -0.33$) clearly indicate that the existence of the BS with $\Delta z_{MR} \geq 0.25h_d$ leads to the development of the 3D flow within the

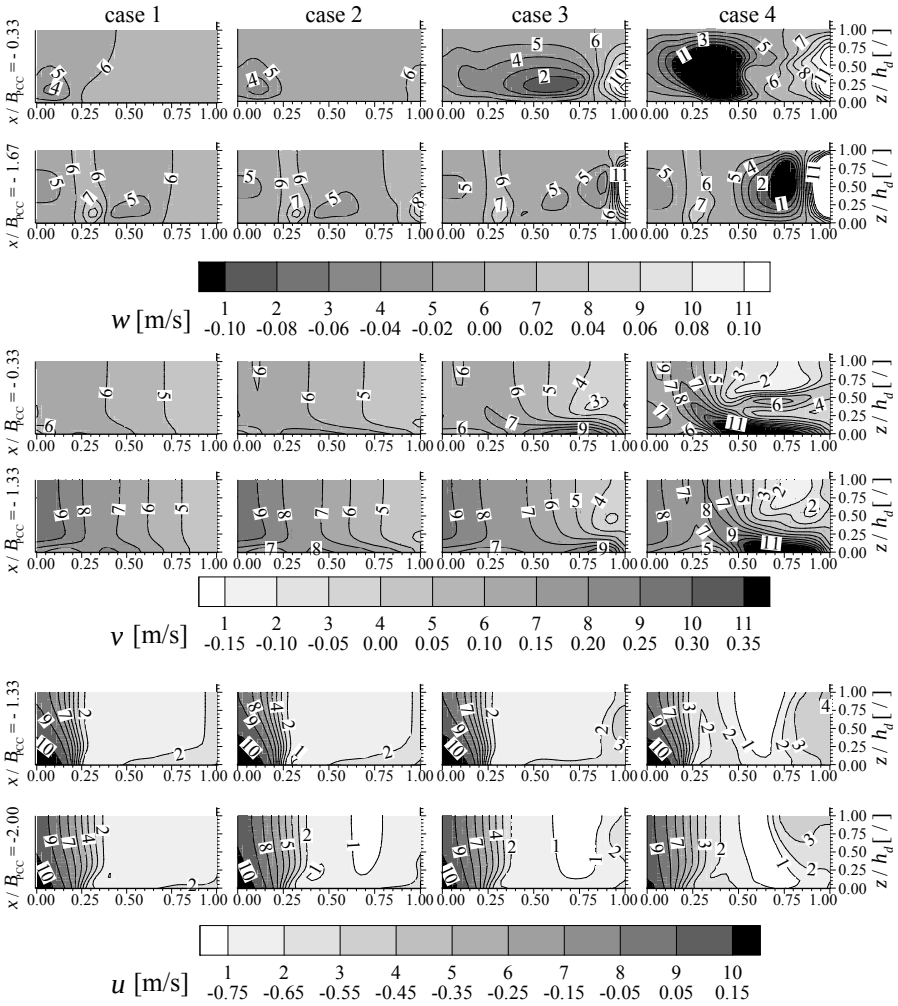

Figure 5. Effects of bed elevation discordance in the main-canal on cross-sectional distributions of three velocity components in the confluence ($x/B_{PCC} = -0.33$) and downstream of the confluence ($x/B_{PCC} = -1.33$ and $x/B_{PCC} = -2.00$), see Figure 1

confluence. The higher the step is, the stronger is the 3D flow, i.e. the greater are magnitudes of the w and v velocities. The w-velocity reaches the same order of magnitude as the velocity $V_{xy} = (u^2 + v^2)^{1/2}$ on the horizontal plane, which is consistent with the experimental findings of Best and Roy [2] and Bradbrook *et al*. [3] in the confluences of parallel canals. The apparent termination of streamlines at the vertical step face and at the opposite wall in case 4 (Fig. 4), means that the fluid continues moving vertically along these surfaces. The strong upward movement along the opposite wall extends far downstream of the confluence ($x/B_{PCC} < -1.67$). Thus, the stability of the river bank, which rests on the opposite side of the confluence, is endangered by erosion. The continuation of the tributary flow along the BS-face ($z < \Delta z_{MR}$) towards this wall is visible on the v-velocity distributions. The magnitude of the v-velocity is here 4 – 5 times greater than that of the stream-wise component u (not presented in Fig. 5, due to limited space).

The enhancement of the 3D flow in the confluence due to the presence of the BS in the main canal affects u-velocity distributions in the following. The core of u_{max} reduces with the increase in Δz_{MR}.

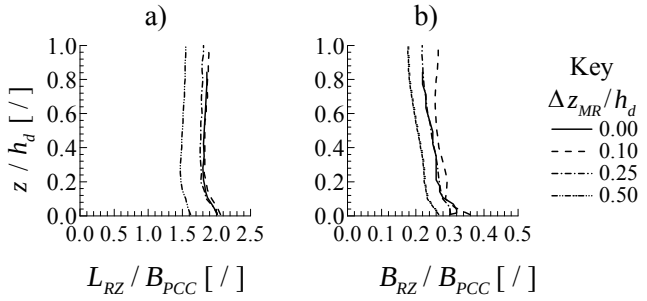

Figure 6. Effect of bed elevation discordance in the main-canal on the RZ size; variations of non-dimensional RZ: a) length and b) width throughout the flow depth

The core occupies approximately $0.75B_{PCC}$ when $\Delta z_{MR} \leq 0.10h_d$. However, as Δz_{MR} increases above $0.25h_d$, its size is significantly reduced (for $\Delta z_{MR} = 0.50h_d$ it occupies $0.25B_{PCC}$), it is moved away from the junction-side wall to the other half of the cross-section ($y/B_{PCC} > 0.50$) and isovels that delineate u_{max}-core are no longer vertical lines, which is consistent with the increase in the area with large *w*-velocities along the opposite wall.

One can also trace the size of the RZ in cross-sectional *u*-velocity distributions. The reduction of the core of positive *u*-velocities (i.e. velocities that are directed upstream) in one cross-section, for example in $x/B_{PCC} = -2.00$, with the increase in $\Delta z_{MR}/h_d$ indicates that the size of the RZ reduces.

Recirculation zone. Figure 6 presents variations of the RZ length and its maximal width through the flow depth. It can be noticed that for this particular D_R-value the presence of the BS with $\Delta z_{MR} \leq 0.25h_d$ practically has no influence on the RZ length. However, this does not hold for the RZ maximal width – the BS with $\Delta z_{MR} = 0.10h_d$ leads to its gradual narrowing from the bottom towards the free-surface. When $\Delta z_{MR} = 0.50h_d$ the zone is systematically shortened and narrowed throughout the flow depth by 20%. This means that the shape of the zone is preserved, but the size is reduced (Fig. 4).

CONCLUSIONS

Flow characteristics in a 90º straight-canals' confluence with the backward facing step at the entrance of the main-canal to the confluence were studied numerically using the 3D finite-volume based model. Only the hydrological scenario with almost equal discharge contributions of the converging canals was analysed. Four values of the bed elevation discordance ratio, including the concordant beds' case $\Delta z_{MR} = 0.00$ were studied: $\Delta z_{MR}/h_d = \{0.00, 0.10, 0.25, 0.50\}$. The numerical simulation results have shown the following.

1. The vertical bed-step, whose face lies in the continuation of the tributary wall, helps that part of the tributary flow which is passing near the upstream junction corner to keep its original direction in the bottom layers. Moreover, a large pressure drop, which develops in front of the bed-step, withdraws a portion the tributary flow towards the bed-step when $\Delta z_{MR} = 0.50h_d$.
2. The presence of the bed-step suppresses 3D flow at the tributary entrance to the confluence below the step-crest. Strong downward oriented 3D flow ($|\varphi| > 20º$) exists at elevations above the crest-level only along the upstream part of the junction-line ($l \leq 0.50L_{u\text{-}d}$). Although the φ-angle changes its sign along the downstream half of the junction line, the flow in this part of the downstream tributary cross-section can be considered as 2D, because $\varphi \approx 0º$.

3. The lateral velocity component v is 4−5 times greater than the stream-wise component u in the confluence when $\Delta z_{MR} \geq 0.25h_d$. Additionally, the vertical velocity w reaches the same order of magnitude as the horizontal velocity V_{xy}, which means that there is a strong 3D circulation within the confluence.
4. Large upward w-velocities develop along the opposite wall. They exist far downstream of the confluence ($3-5B_{PCC}$), meaning that this bank is endangered by the erosion. Large downward velocities in the confluence, on the other hand, create conditions for deepening of the scour hole within the confluence.
5. The presence of the bed-step in the main-canal does not affect the shape of the recirculation zone when $\Delta z_{MR} \geq 0.25h_d$. The size of the RZ is almost completely preserved for $\Delta z_{MR} = 0.25h_d$. However, the RZ is systematically reduced by 20% when $\Delta z_{MR} = 0.50h_d$.
6. Very low bed-steps ($\Delta z_{MR} \leq 0.10h_d$) do not affect the RZ length, but they cause its gradual narrowing towards the free-surface.

REFERENCES

[1] Best J.L., "Sediment transport and bed morphology at river channel confluences", *Sedimentology*, Vol. 35, (1988), pp 481-498.

[2] Best J.L. and Roy A.G. , "Mixing-layer distortion at the confluence of channels of different depth", *Nature*, Vol. 350, (1991), pp 411-413.

[3] Bradbrook K.F., Biron P., Lane S.N., Richards K.S. and Roy A.G., "Investigation of controls on secondary circulation in a simple confluence geometry using a three-dimensional numerical model", *Hydrological Processes*, Vol. 12, (1998), pp 1371-1396.

[4] De Serres B., Roy A.G., Biron P.M. and Best J.L., "Three-dimensional structure of flow at a confluence of river channels with discordant beds", *Geomorphology*, Vol. 26, (1999), pp 313-335.

[5] Đorđević D., "*Numerical investigation of the river confluence hydrodynamics*", Unpublished PhD Dissertation, University of Belgrade, Belgrade, 382p, (2010).

[6] Đorđević D., "Numerical study of 3D flow at right-angled confluences with and without upstream planform curvature", *J. of Hydroinformatics*, Vol. 15.4, (2013), pp 1073-1088.

[7] Đorđević D., "*Controls of three-dimensional flow at river confluences*" (bilingual – in Serbian and in English), Beograd, Zadužbina Andrejević, (2013).

[8] Gaudet J.M. and Roy A.G., "Effect of bed morphology on flow mixing length at river confluences", *Nature*, Vol. 373, (1995), pp 138-139.

[9] Huang J., Weber L. J. and Lai Y. G., "Three-dimensional study of flows in open-channel junctions", *J. Hydraulic Engineering*, ASCE, Vol.128, No.3, (2002), pp 268-280.

[10] Kennedy B., "On Playfair's law of accordant junctions", *Earth Surface Processes and Lanforms*, Vol. 9, (1984), pp 153-173.

[11] Mosley M. P., "An experimental study of channel confluences", *Journal of Geology*, Vol. 94, (1976), pp 535-562.

[12] Olsen N.R., "*CFD Algorithms for Hydraulic Engineering*", Trondheim, The Norwegian University of Science and Technology, (2000).

[13] Shumate E.D., "*Experimental description of flow at an open-channel junction*", Unpublished Master thesis, Univ. of Iowa, Iowa, 150 p, (1998).

[14] Weerakoon S.B., Tamai N. and Kawahara Y., "Bed topography, bed shear stress distribution and velocity field in a confluence", *Proc. of Hydraulic Engineering*, JSCE, Vol.34, (1990), pp 307-312.